

Enhancement of physicochemical properties of polyurethane-perovskite nanocomposite *via* addition of nickel titanate nanoparticles

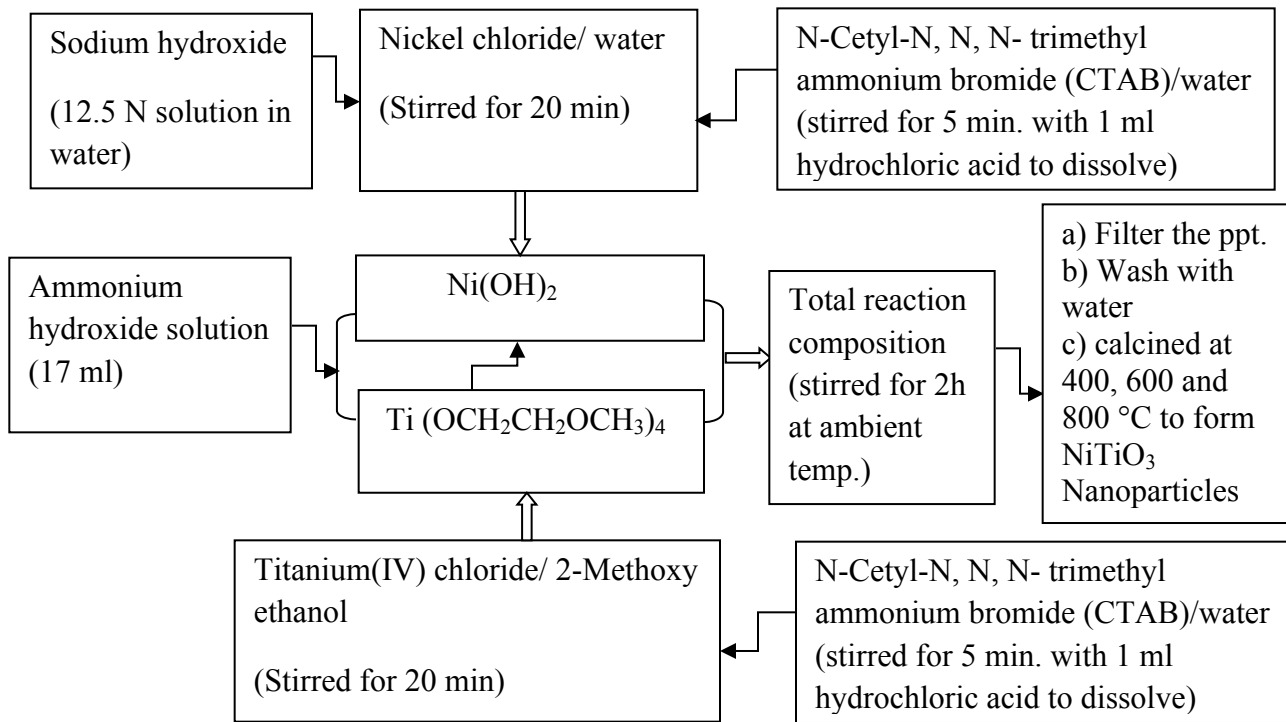
Adhigan Murali,^a Senthil A. Gurusamy-Thangavelu,^{a,*} Sellamuthu N. Jaisankar^{a,*} and Asit Baran Mandal^{a,b*}

^aPolymer Division, ^bChemical laboratory, Council of Scientific and Industrial Research (CSIR)-CLRI, Adyar, Chennai-600020, India *E-mail: senthil@clri.res.in; snjsankar@clri.res.in; abmandal@clri.res.in; Tel: 91-44-24422059; Fax: 91- 44-24911589.

Contents	page #
Schematic outline of nickel titanate synthesis by co-precipitation method	S3
Fig. S1 Raman spectrum of NiTiO ₃ (after thermal treatment at 600 ° C)	S4
Fig. S2 TGA shows the degradation of NiTiO ₃ NPs from 25 to 800 °C.	S5
Fig. S3 Optical microscope image of NiTiO ₃ nanoparticles	S6
Fig. S4 SEM images of control PU, NiTiO ₃ NPs and PU-NiTiO ₃ nanocomposite	S7
Fig. S5 AFM image of NiTiO ₃ NPs with height and width profile	S8
Fig. S6 AFM image of NiTiO ₃ NPs with phase profile	S9
Fig. S7 AFM image of NiTiO ₃ NPs with height profile	S10
Fig. S8 AFM image of NiTiO ₃ NPs with roughness (R_q) profile	S11
Fig. S9 AFM image of PU-NiTi800 film distributed with NiTiO ₃ NPs	S12
Fig. S10 AFM image of PU-NiTi800 film, NiTiO ₃ NPs probed on its surface	S13
Fig. S11 AFM image of PU-NiTi800 film with roughness (R_q) profile	S14
Fig. S12 AFM image of PU-NiTi800 nanocomposite film 3D surface	S15

Fig. S13 AFM image of PU-NiTi800 nanocomposite film 3D surface	S16
Fig. S14 AFM image of PU-NiTi800 nanocomposite - 3D topography	S17
Fig. S15 Tensile profile of control PU	S18
Fig. S16 Tensile profile of PU nanocomposite, PU-NiTi400	S19
Fig. S17 Tensile profile of PU nanocomposite, PU-NiTi600	S20
Fig. S18 Tensile profile of PU nanocomposite, PU-NiTi800	S21
Fig. S19 DSC profile of PU and PU-NiTiO ₃ films (expanded around the T _g region)	S22
Table. S1 ATR-IR data of PU and PU-NiTiO ₃ nanocomposite films	S23
References	S23

Schematic outline of nickel titanate synthesis by co-precipitation method



Scheme S1. Synthesis of nickel titanate NPs by co-precipitation method at 400, 600 and 800 ° C.

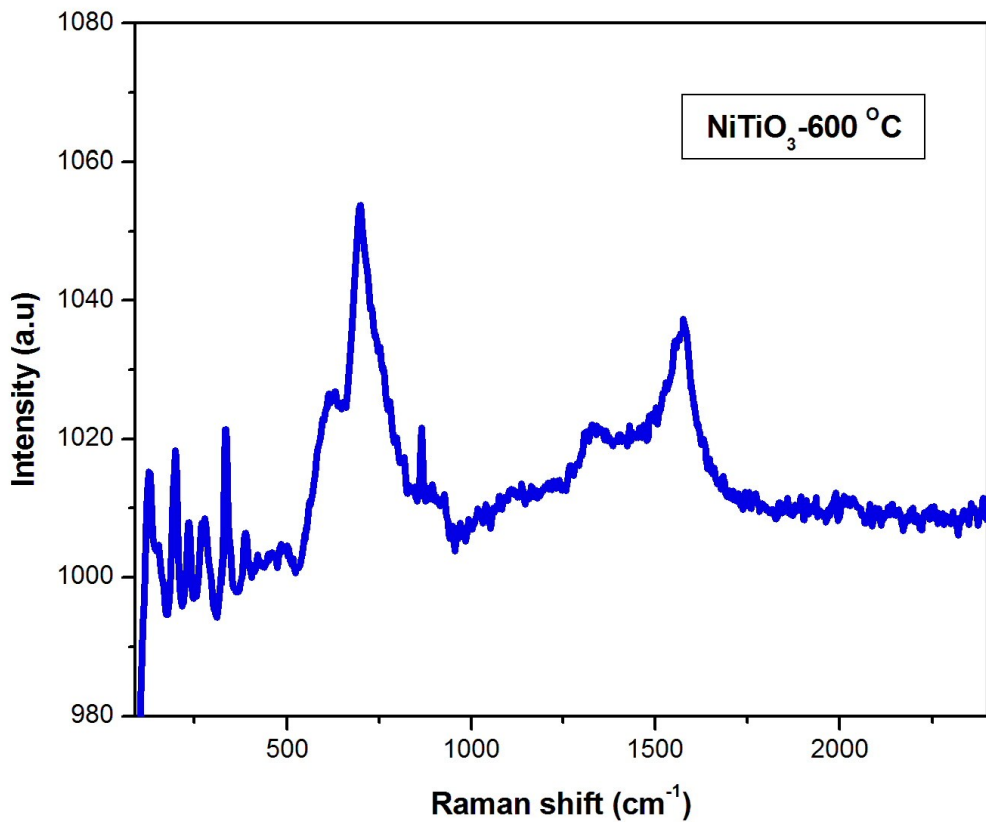


Fig. S1. Raman spectrum depicts the formation of NiTiO_3 , after calcinated for 4 h at $600\text{ }^{\circ}\text{C}$.¹

Sample: SAMPLE-800
Size: 9.6020 mg
Method: 10
Comment: SAMPLE-800

TGA

File: F:\...\TGAINITIO3 600,800\SAMPLE-800.001
Operator: EDWIN PAUL
Run Date: 13-Oct-2014 12:36
Instrument: TGA Q50 V20.13 Build 39

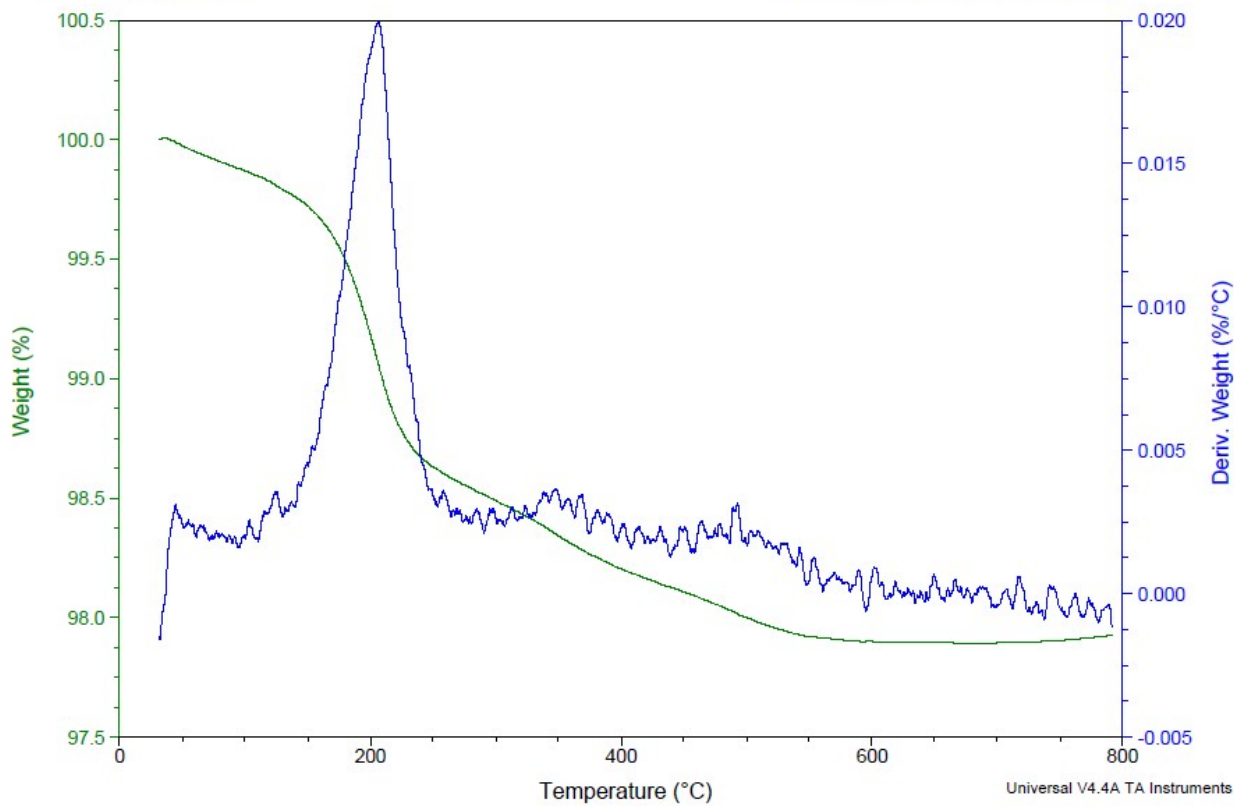


Fig. S2. TGA shows the degradation of NiTiO_3 NPs from 25 to 800 °C.

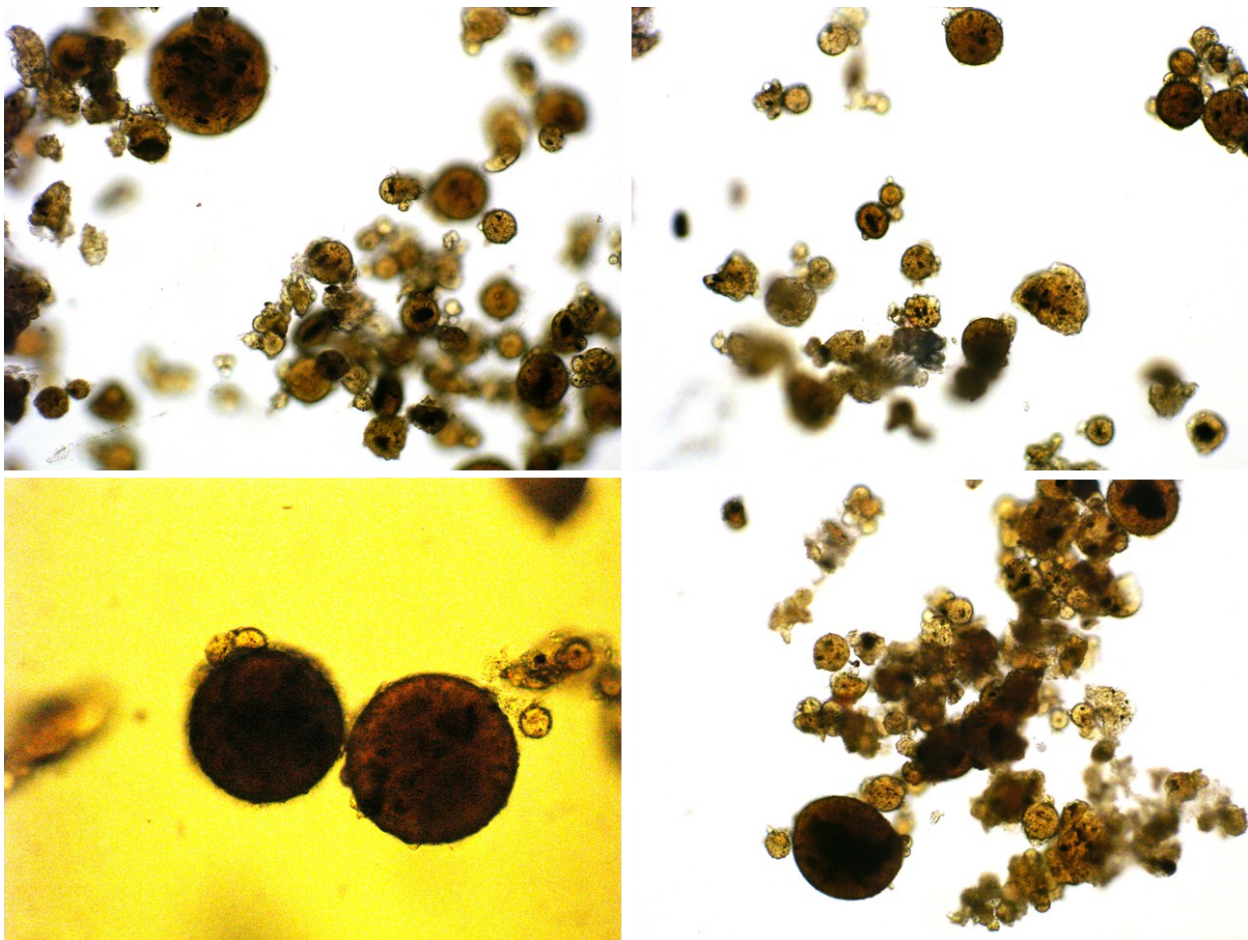


Fig. S3. Optical images of NiTiO₃ nanoparticles after calcinated at 800 °C (50 X).

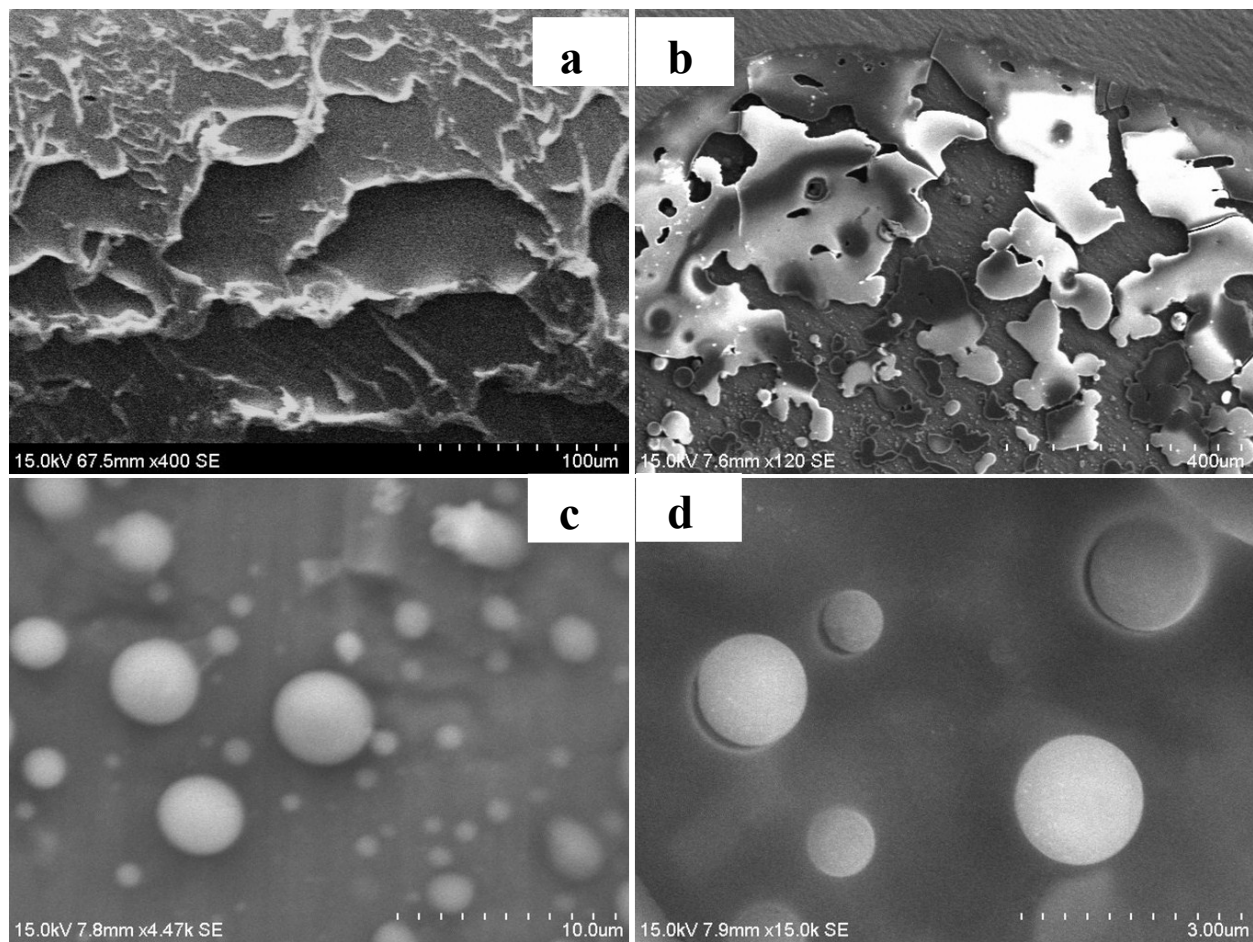


Fig. S4. SEM images of samples a) control PU film b) PU- NiTiO₃ nanocomposite film
c) NiTiO₃ NPs calcinated at 800 °C and d) magnified image of NiTiO₃ NPs.³

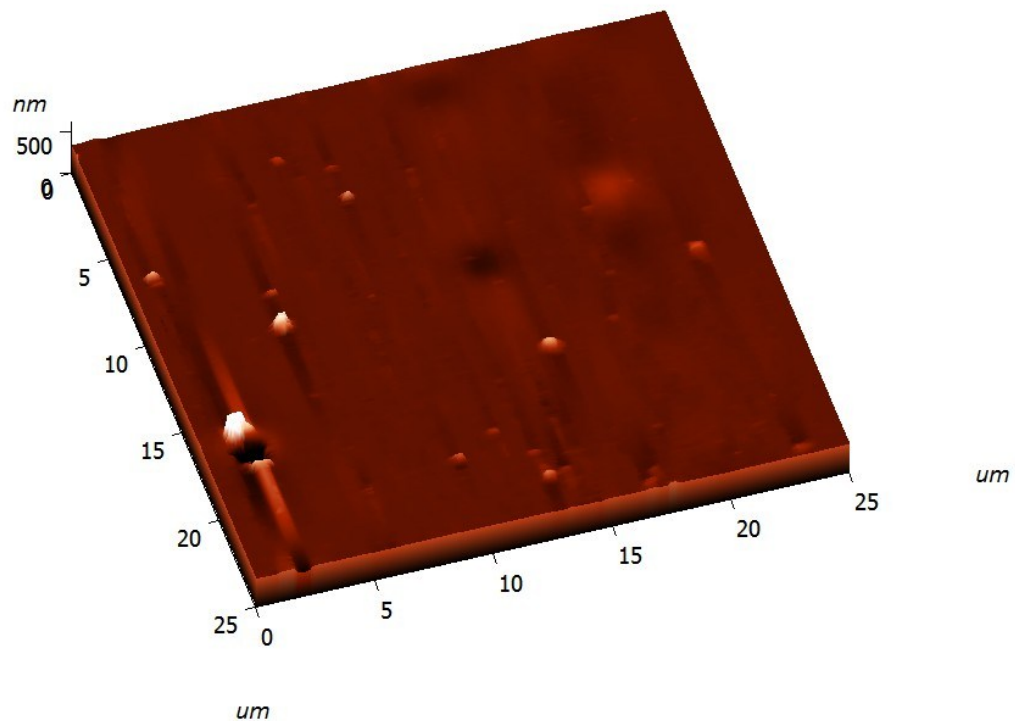


Fig. S5. AFM image of NiTiO₃ NPs with height and width profile.⁴

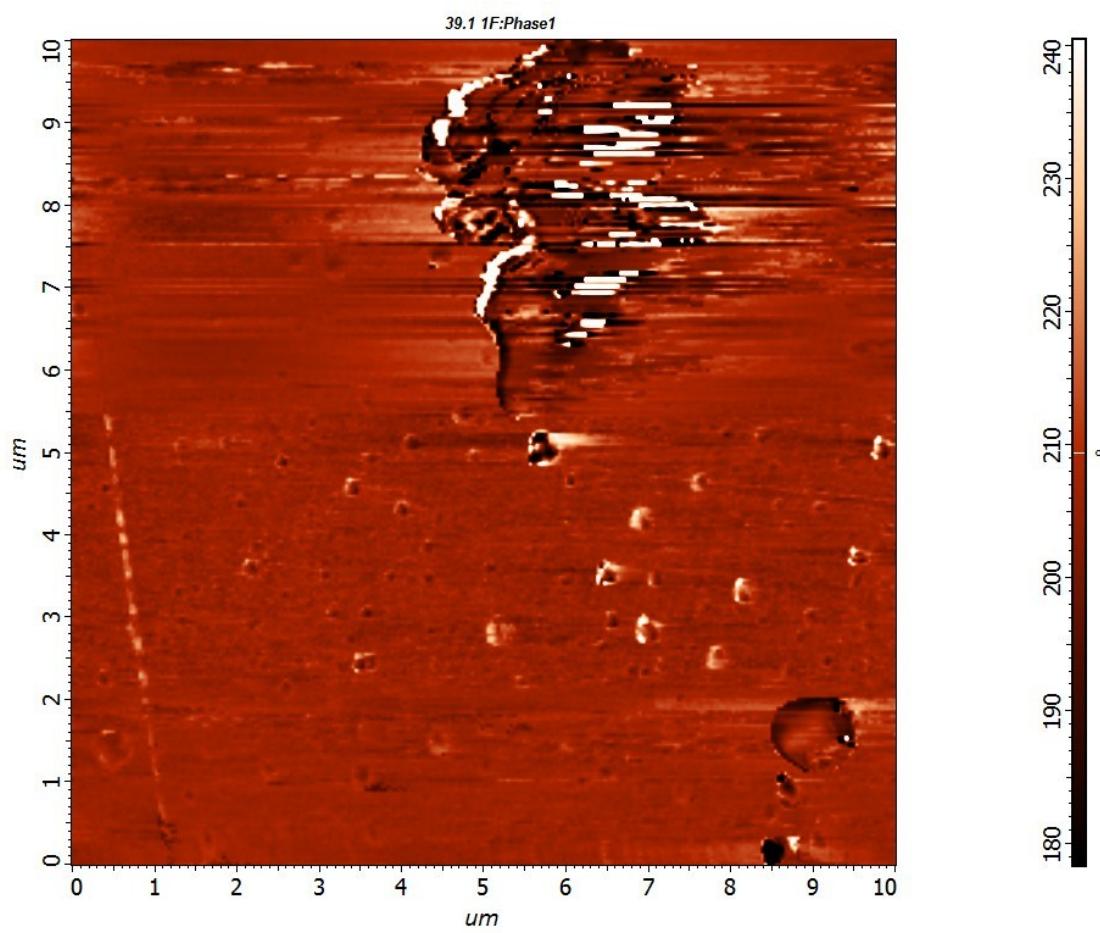


Fig. S6. AFM image of NiTiO_3 NPs with phase profile.

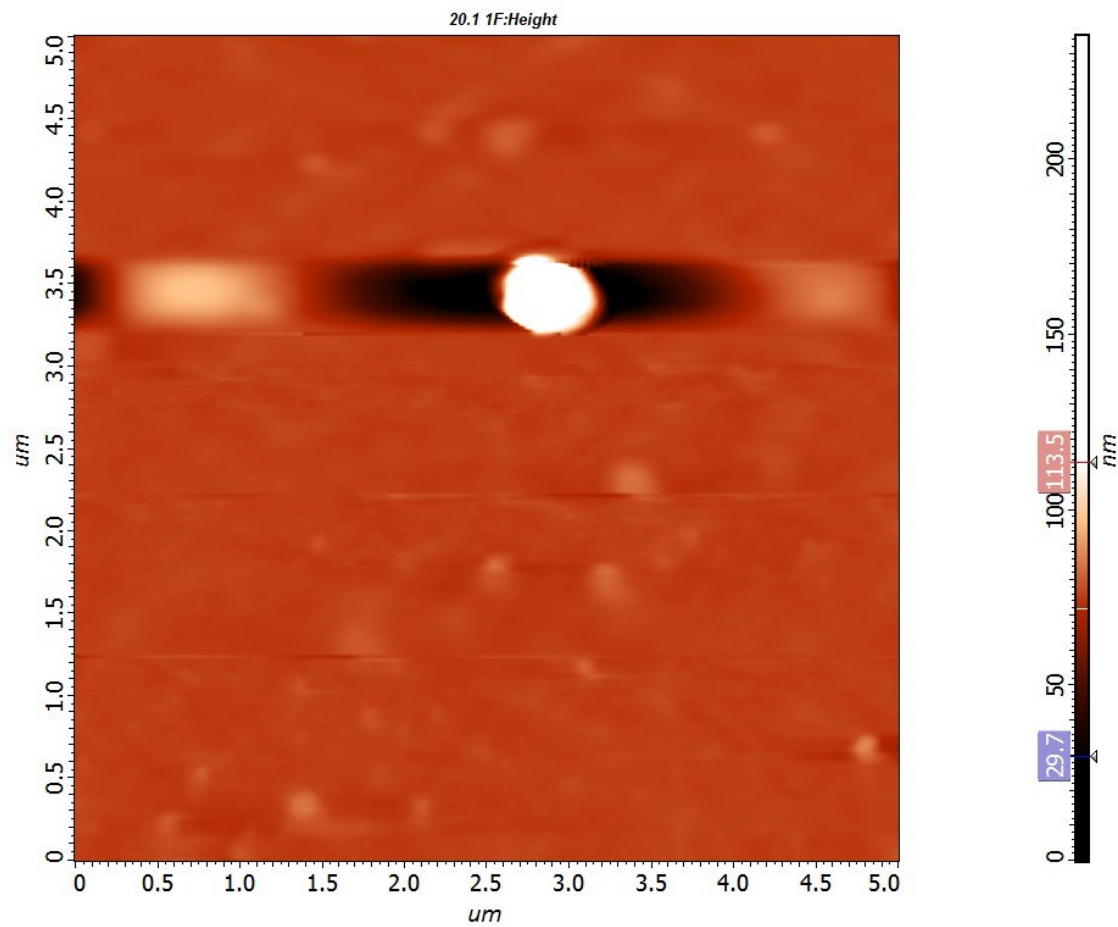


Fig. S7. AFM image of NiTiO_3 NPs with height profile.

4.3 1F:Height profile. Roughness profile

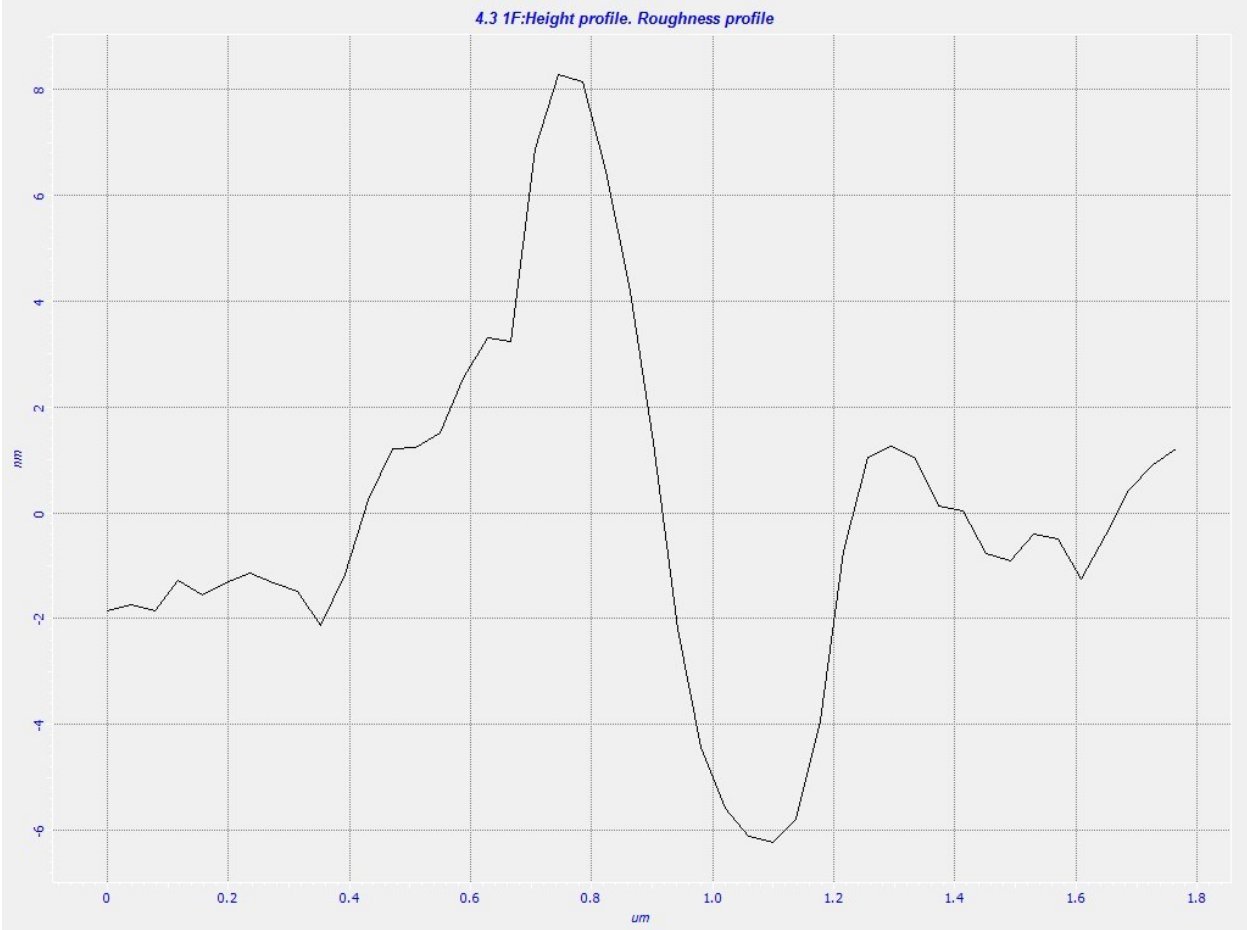


Fig. S8. AFM image of NiTiO₃ NPs with roughness (R_q) profile.⁵

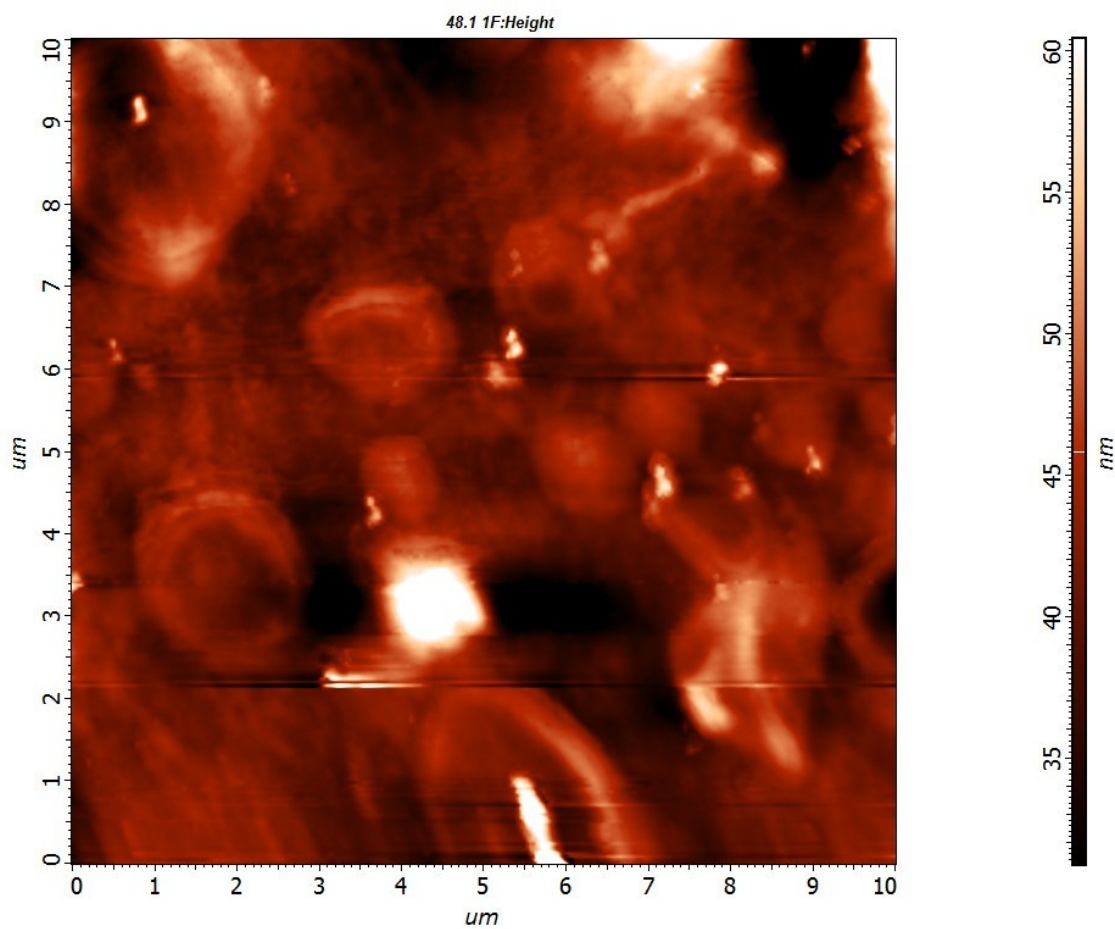


Fig. S9. AFM image of PU-NiTi800 film distributed with NiTiO_3 NPs.

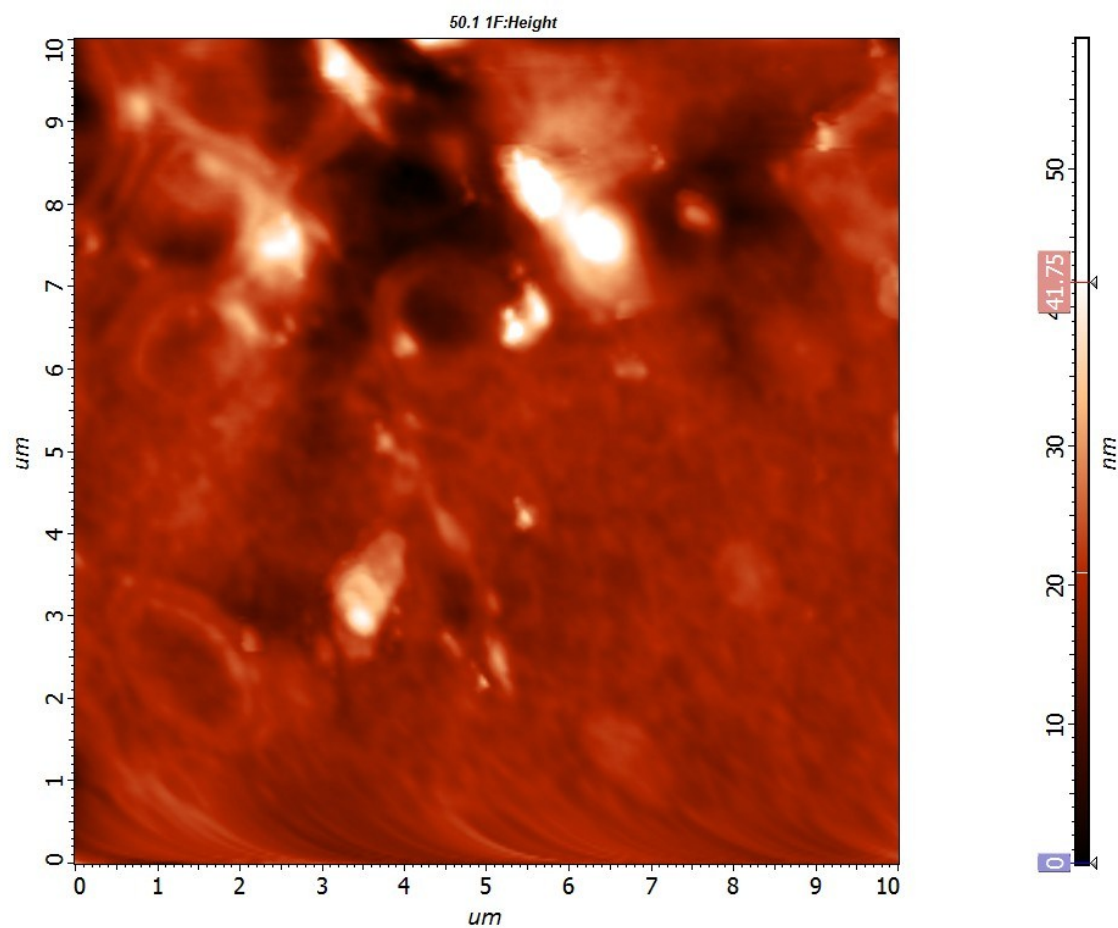


Fig. S10. AFM image of PU-NiTi800 film, NiTiO₃ NPs probed on its surface.

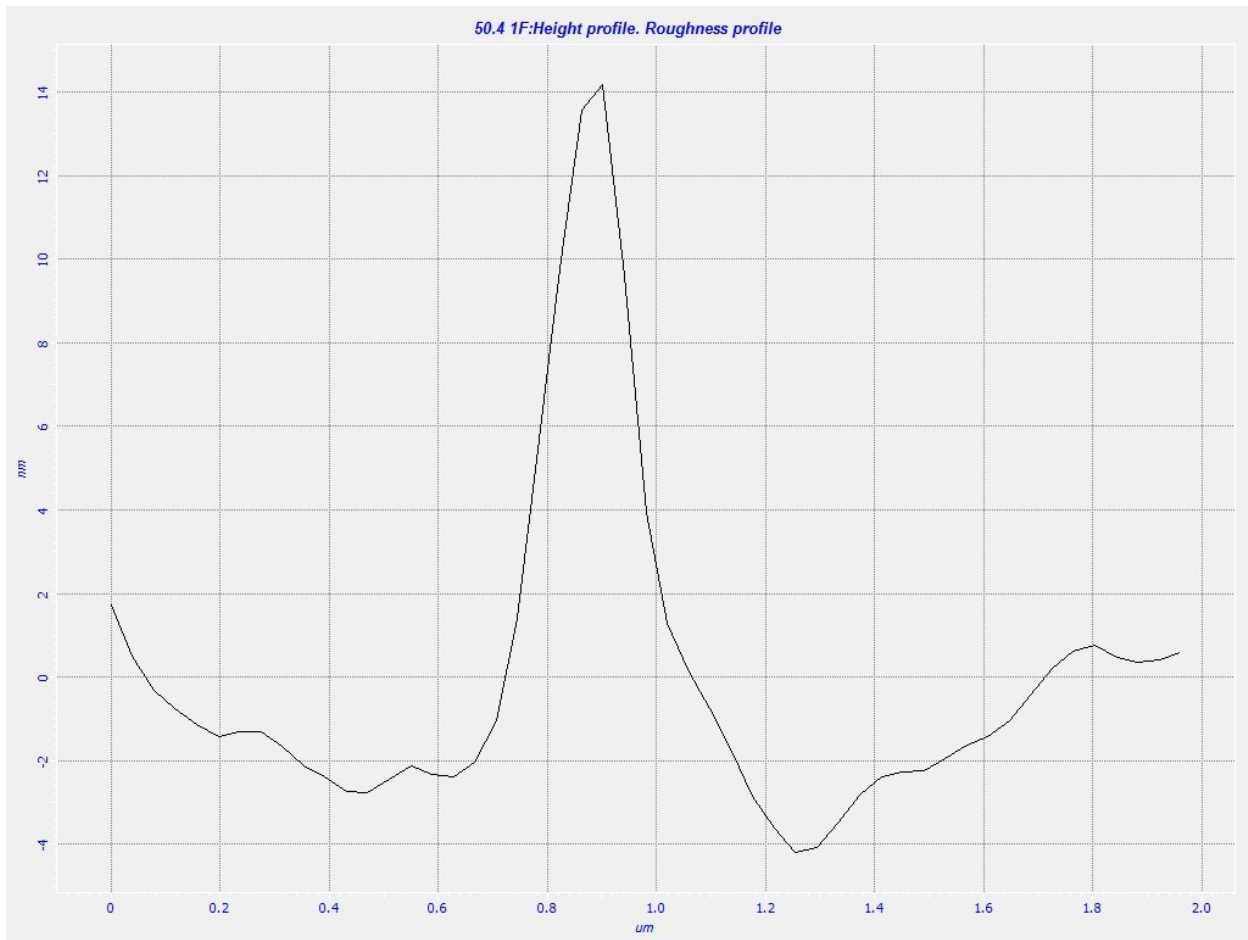


Fig. S11. AFM image of PU-NiTi800 film with roughness (R_q) profile.⁶

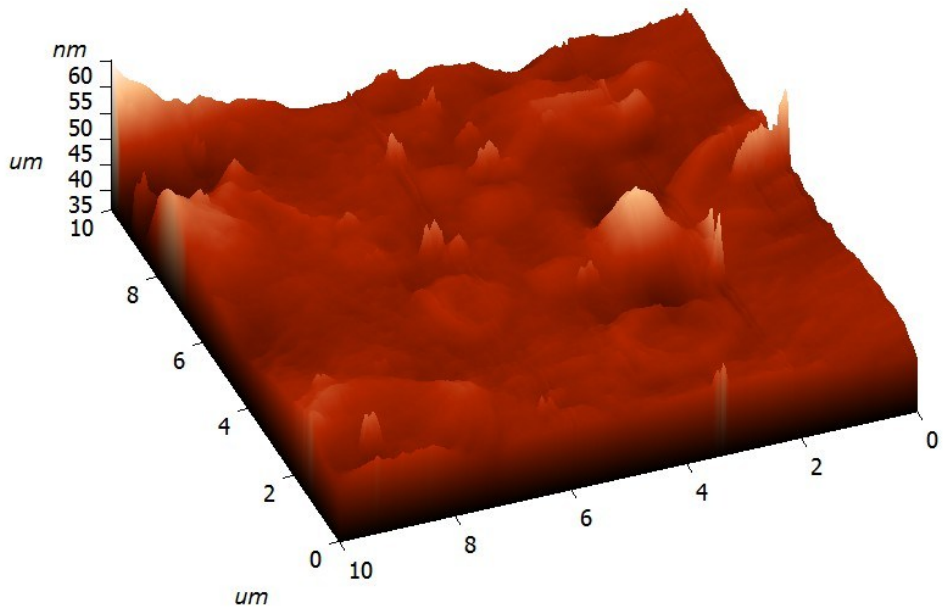


Fig. S12. AFM image of PU-NiTi800 nanocomposite film - 3D surface profile.

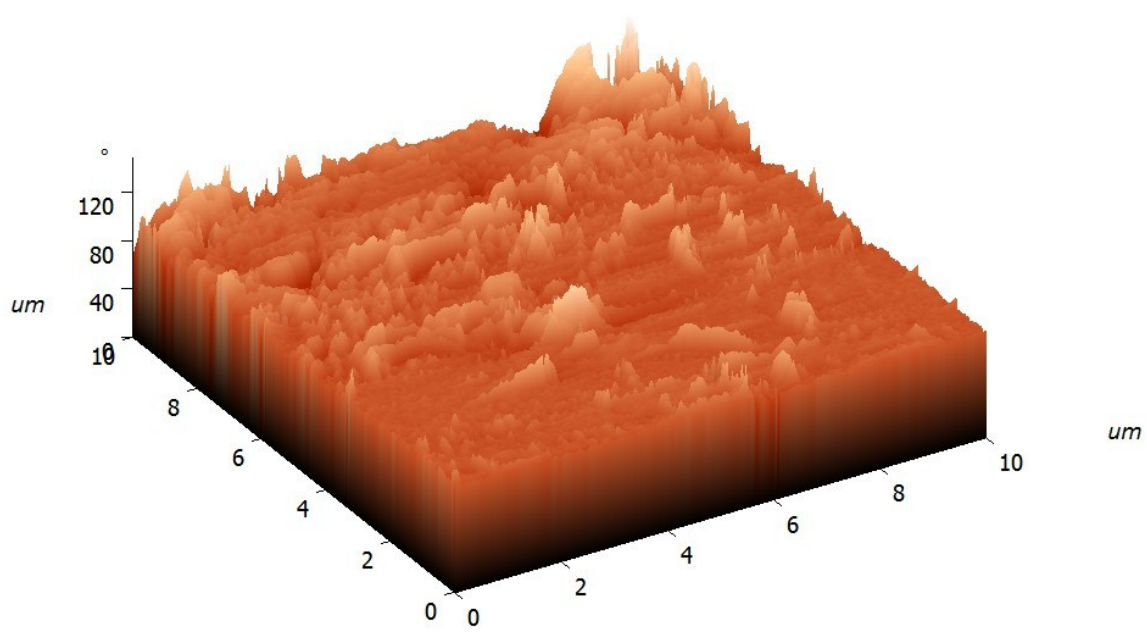


Fig. S13. AFM image of PU-NiTi800 nanocomposite film - 3D surface profile.

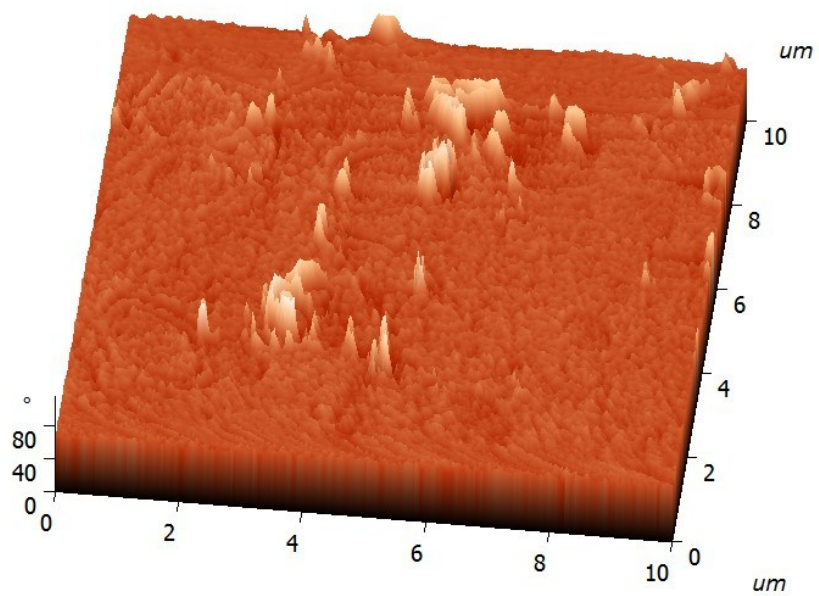


Fig. S14. AFM image of PU-NiTi800 nanocomposite film - 3D topography.

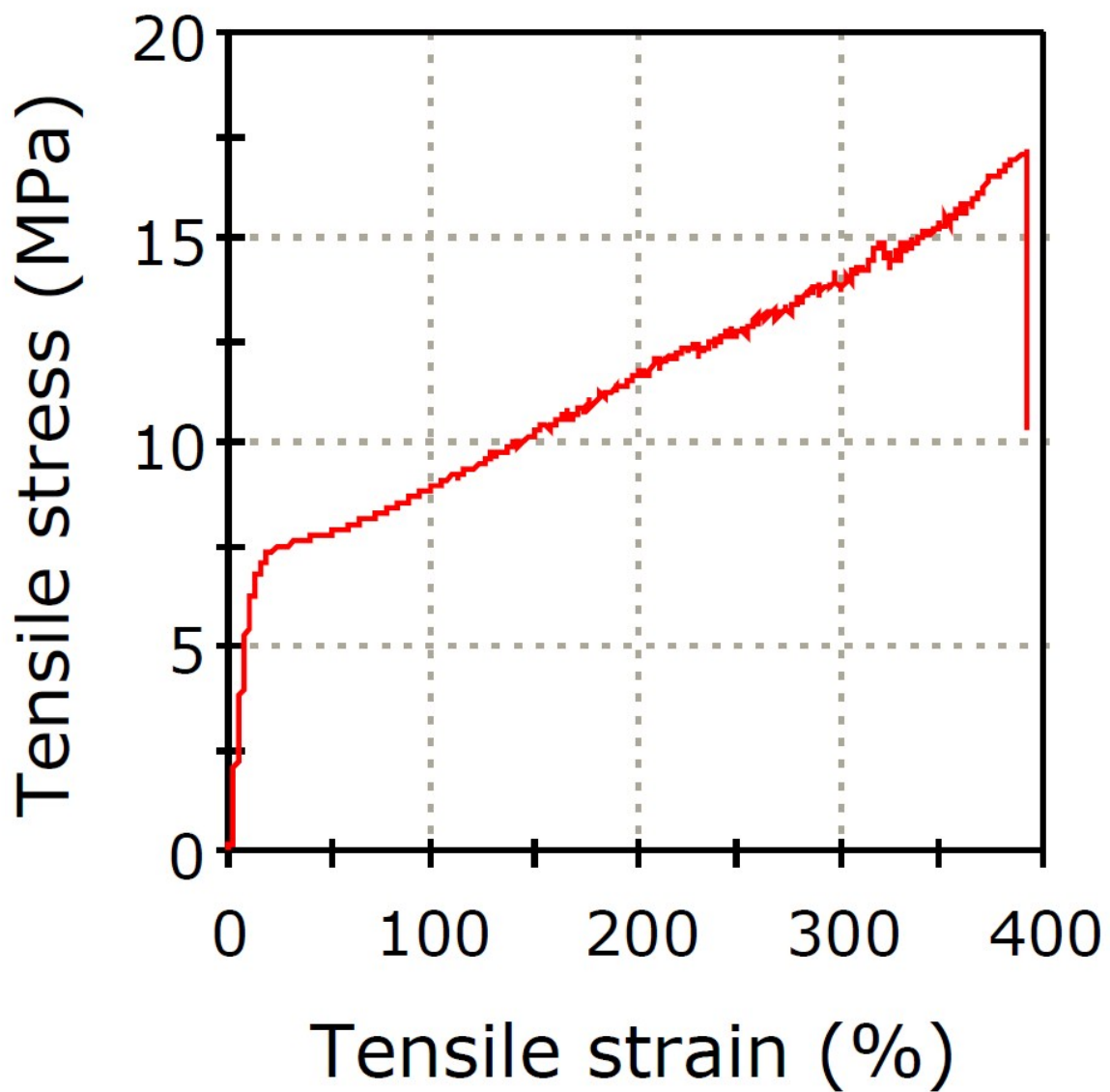


Fig. S15. Tensile profile of control PU film.

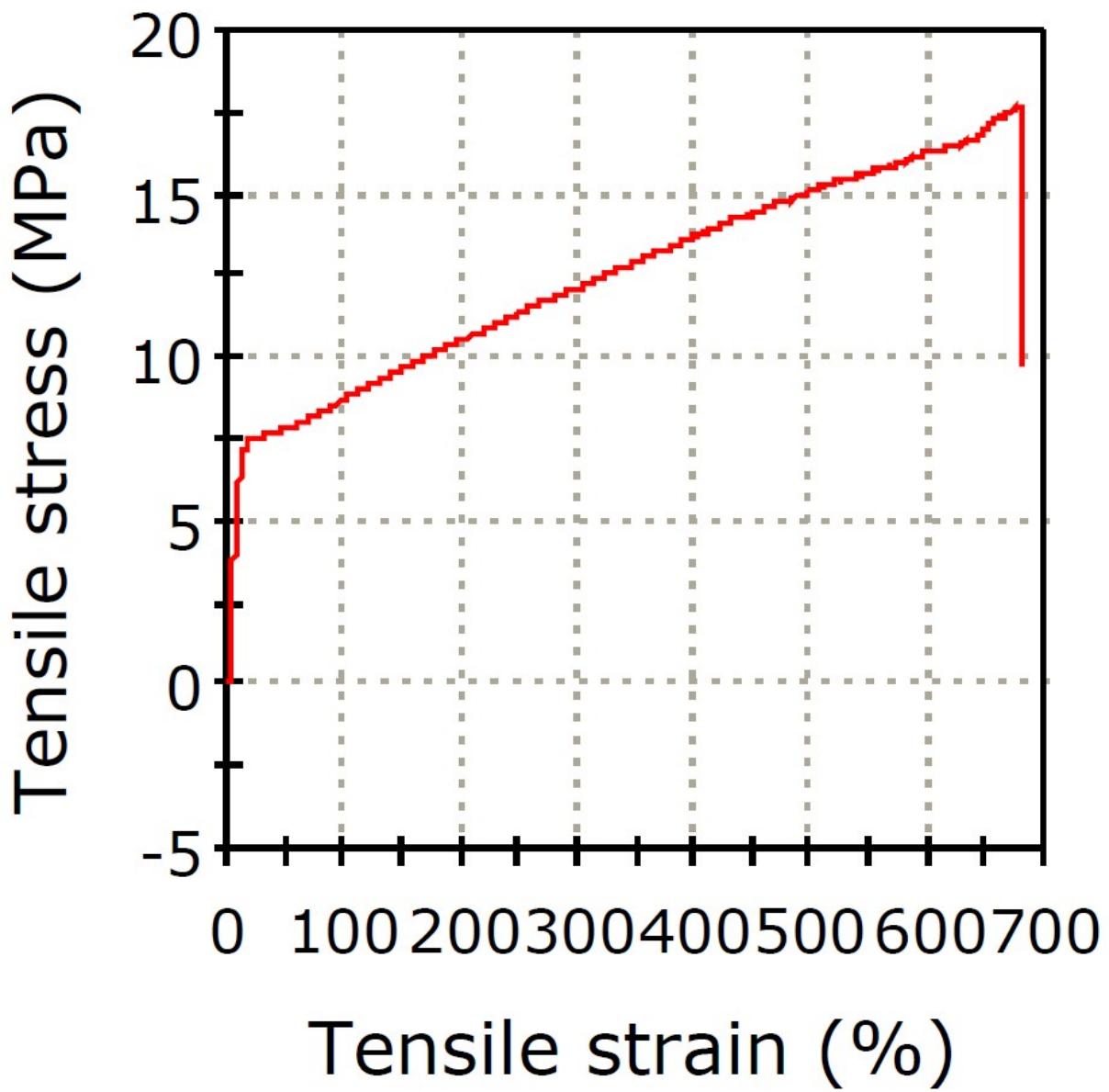


Fig. S16. Tensile profile of PU nanocomposite film, PU-NiTi400.

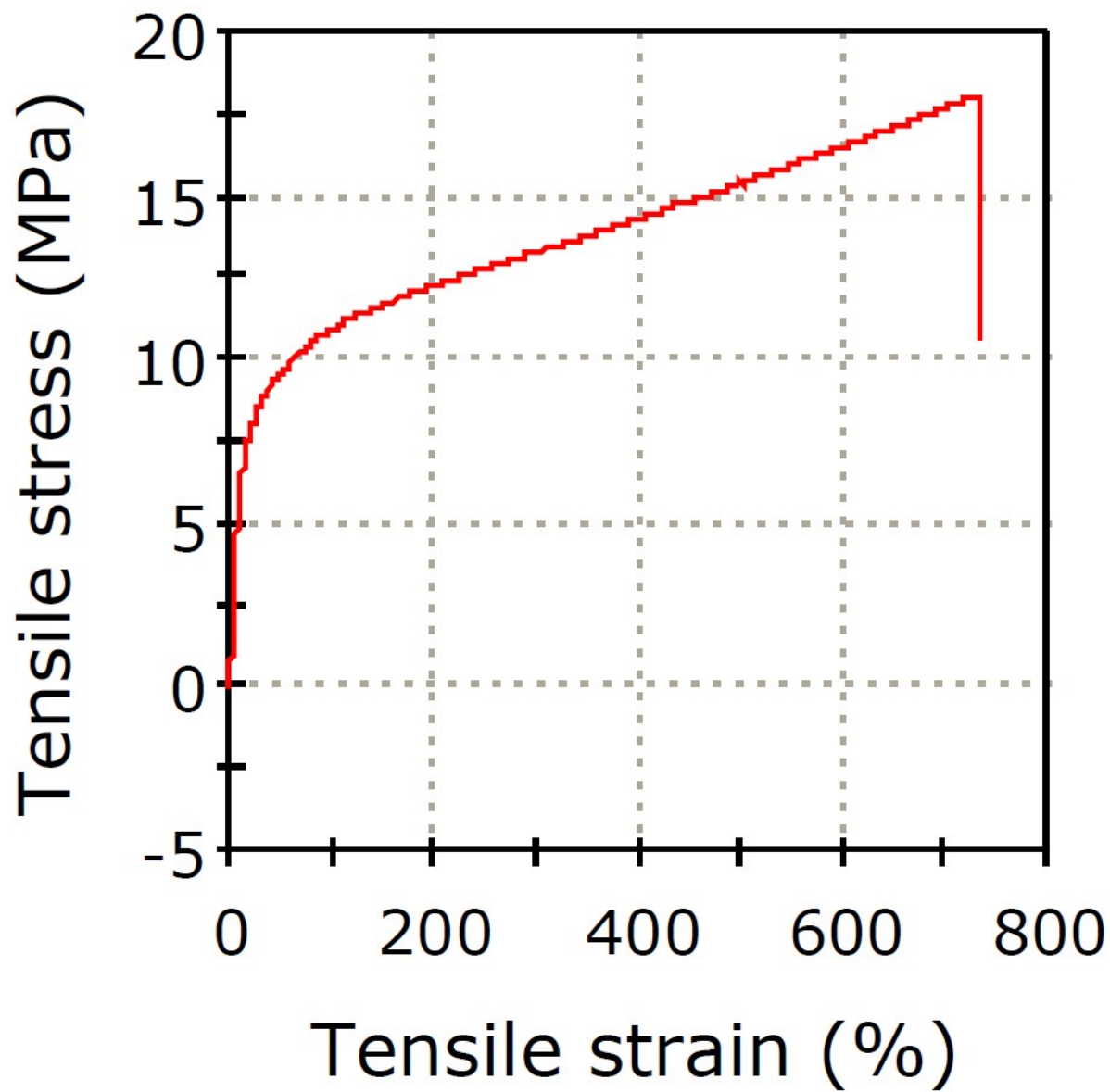


Fig. S17. Tensile profile of PU nanocomposite film, PU-NiTi600.

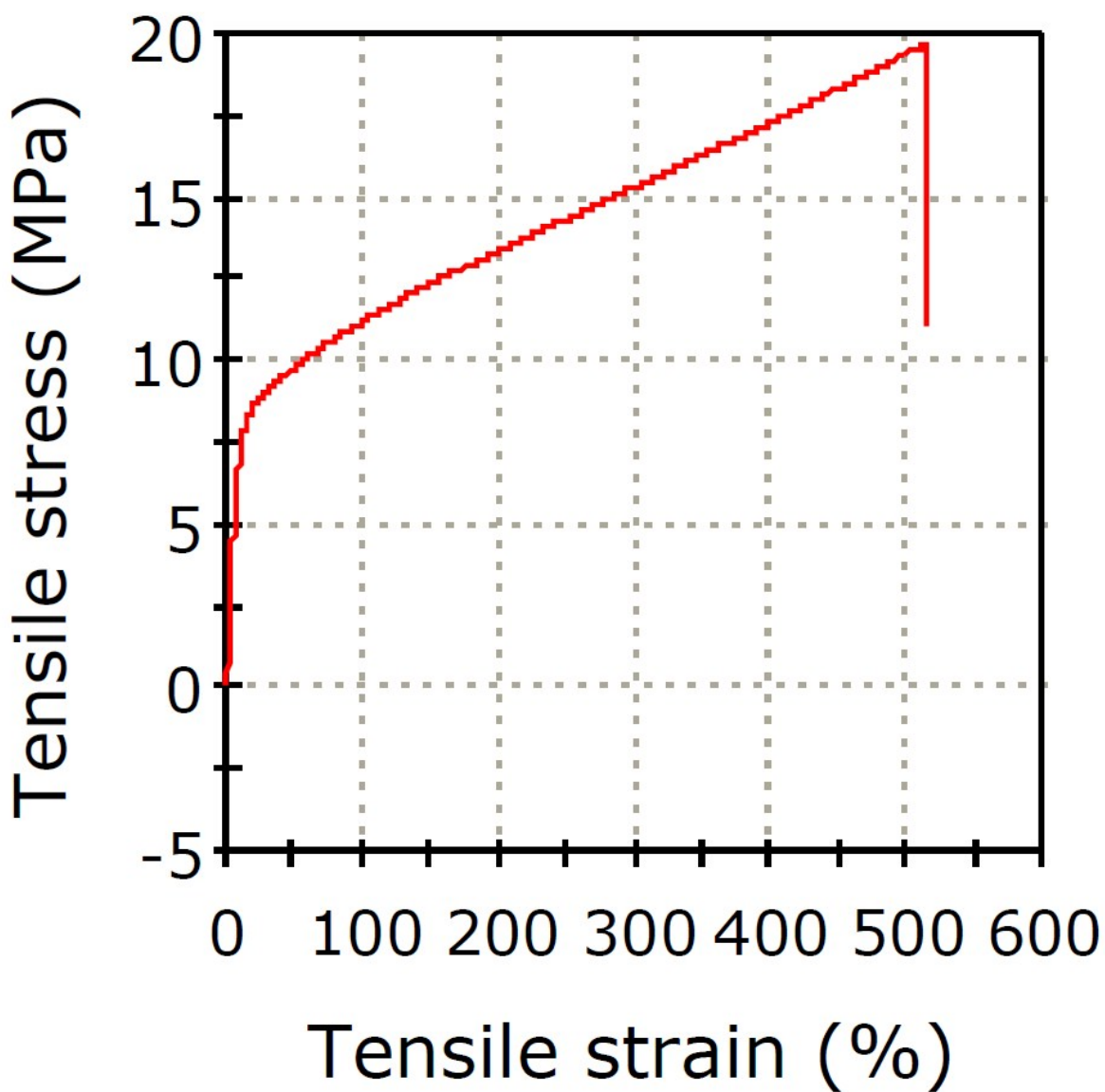


Fig. S18. Tensile profile of PU nanocomposite film, PU-NiTi800.

In mechanical properties study, first one third region of the tensile profile provides information about elastic deformation and the remaining region corresponds to ductile deformation.⁷ PU-NiTiO₃ nanocomposite samples, PU-NiTi600 and PU-NiTi800 are deduced to exhibit plastic behavior, since the stress-strain curve passes through strain hardening region, which is above the steady state and critical stress.

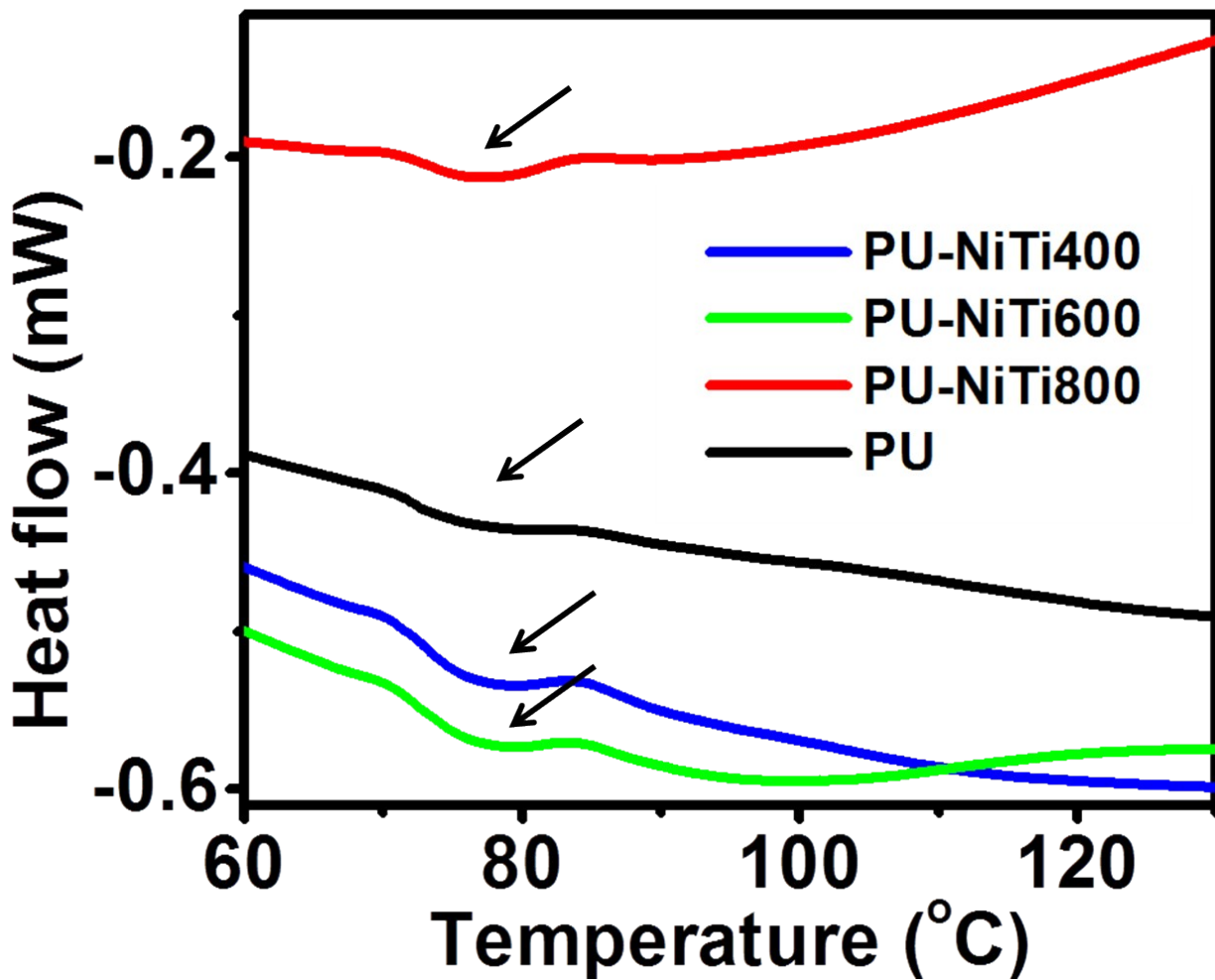


Fig. S19. DSC profile of PU and PU- NiTiO_3 films (expanded around the T_g region).

Table S1. ATR-IR data of PU and PU-NiTiO₃ nanocomposite films.

S. No.	Sample codes	Urethane (-NH-) [cm ⁻¹]	Urethane (-CO-) [cm ⁻¹]	PPG Methyl (-C-H) [cm ⁻¹]	PPG skeleton (C-O-C) [cm ⁻¹]
1	PU	3310	1720	2980	1095
2	PU-NiTi400	3300	1705	2975	1082
3	PU-NiTi600	3014	1652	3011	1086
4	PU-NiTi800	3283	1639	2947	1094

References:

1. Chuang, S. H.; Hsieh, M. L.; Wang, D. Y. *J. Chin. Chem. Soc.* **2012**, *59*, 628.
2. Traistaru, G. A.; Covaliu, C. I.; Matei, V.; Cursaru, D.; Jitaru, I. *Dig. J. Nanomater. Bios.* **2011**, *6*, 1257.
3. Dias, R. C. M.; Góes, A. M.; Serakides, R.; Ayres, E.; Oréfice, R. L. *Mater. Res.* **2010**, *13*, 211.
4. Gélinas, V. Vidal, D. *Powder Technol.* **2010**, *203*, 254.
5. Miller, J. D.; Veeramasuneni, S.; Drelich, J.; Yalamanchili, M. R.; Yamauchi, G. *Polym. Eng. Sci.* **1996**, *36*, 1849.
6. Seen Meera, K. M.; Murali Sankar, R.; Jaisankar, S. N.; Mandal, A. B. *J. Phys. Chem. B*, **2013**, *117*, 2682.
7. Tullis, T. E.; Tullis, J. *Geophys. Monogr.* **1986**, *36*, 297.